Forest Ecology and Management 585 (2025) 122645

Contents lists available at ScienceDirect

Forest Ecology and Management

journal homepage: www.elsevier.com/locate/foreco

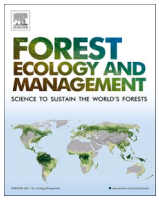

Carbon allocation to roots of suppressed Norway spruce increases immediately after selection harvest

Aleksi Lehtonen [a,*], Juha Heikkinen [a], Chainey A. Boroski [b], Olli-Pekka Tikkasalo [a], Katja T. Rinne-Garmston [a], Elina Sahlstedt [a], Mika Korkiakoski [c], Anna Kärkönen [a,d], Anna Lintunen [e], Harri Mäkinen [a], Mikko Peltoniemi [a], Gonzalo de Quesada [f], Yann Salmon [f], Giles Young [a], Raisa Mäkipää [a], Ram Oren [f,g]

[a] Natural Resources Institute Finland, Latokartanonkaari 9, Helsinki FI-00790, Finland
[b] Duke University, Durham, NC, USA
[c] Finnish Meteorological Institute, Erik Palménin aukio 1, Helsinki FI-00560, Finland
[d] Department of Agricultural Sciences, Viikki Plant Science Centre, University of Helsinki, Helsinki FI-00014, Finland
[e] University of Helsinki, Gustaf Hällströmin katu 2, Helsinki 00014, Finland
[f] University of Helsinki, Latokartanonkaari, 7, Helsinki FI-00014, Finland
[g] Nicholas School of the Environment & Pratt School of Engineering, Duke University, Durham, NC 27708, USA

ARTICLE INFO

Keywords:
Root growth
Continuous-cover forestry (CCF)
Carbon isotope composition ($\delta^{13}C$)
Harvest release effect
Norway spruce
Selection harvest

ABSTRACT

Selection harvesting in fertile, drained peatlands is an alternative for even-aged forestry, where clearcutting takes place at the end of each rotation period. Avoiding clear-cuts has been promoted due to reducing negative externalities, like nutrient loading to waterways and significant greenhouse gas emissions after harvesting. Our aim was to understand the responses of suppressed Norway spruce trees to selection harvesting. We analysed biomass accumulation and priorities of carbon allocation to stems, proximal roots and distal roots. We quantified carbon isotope composition ($\delta^{13}C$) and cross-sectional growth of proximal (supporting) roots and distal (water and nutrient transportation) roots. The study took place in a drained, fertile boreal peatland site in southern Finland, where a selection harvest was conducted in 2016, while an area as a control was left untouched. Our results show that suppressed Norway spruce trees increased their cross-sectional growth of proximal roots and distal roots twice as much as that of the stem during the first five years after the selection harvest. The timing and magnitude of carbon allocation to proximal roots and distal roots were immediate and equal, underlining the fact that trees were investing in mechanical support and nutrient and water uptake. These results show that the climate benefits of selection harvest were not delayed. Instead of immediate growth of stems, we found immediate growth of roots.

1. Introduction

Continuous-cover forestry with selection harvesting has been proposed as a climate change mitigation measure on Norway spruce (*Picea abies*) dominated nutrient-rich drained peatlands because it provides multiple environmental benefits while simultaneously producing timber and revenues for landowners (Juutinen et al., 2021; Lehtonen et al., 2023a; Nieminen et al., 2018). However, this management alternative has also been criticised because it reduces the density of stand throughout the diameter distribution, and suppressed trees may not have the capacity to respond to released competition as well as dominant trees. In a drained peatland forest, the delay in stem diameter growth of suppressed Norway spruce trees ranged from two to five years following selection harvest (Lehtonen et al., 2023b). However, $\delta^{13}C$ of

* Corresponding author.
E-mail addresses: aleksi.lehtonen@luke.fi (A. Lehtonen), juha.heikkinen@luke.fi (J. Heikkinen), chainey.boroski@duke.edu (C.A. Boroski), olli-pekka.tikkasalo@luke.fi (O.-P. Tikkasalo), katja.rinne-garmston@luke.fi (K.T. Rinne-Garmston), elina.sahlstedt@luke.fi (E. Sahlstedt), mika.korkiakoski@fmi.fi (M. Korkiakoski), anna.happonen@luke.fi (A. Kärkönen), anna.lintunen@helsinki.fi (A. Lintunen), harri.makinen@luke.fi (H. Mäkinen), mikko.peltoniemi@luke.fi (M. Peltoniemi), gonzalo.dequesadaalzamora@helsinki.fi (G. de Quesada), yann.salmon@helsinki.fi (Y. Salmon), giles.young@luke.fi (G. Young), raisa.makipaa@luke.fi (R. Mäkipää), ramoren@duke.edu (R. Oren).

https://doi.org/10.1016/j.foreco.2025.122645
Received 9 November 2024; Received in revised form 12 February 2025; Accepted 5 March 2025
Available online 22 March 2025

tree rings suggested that intrinsic water use efficiency (iWUE, i.e., WUE assuming vapour pressure deficit is a constant (Battipaglia et al., 2013; Francey and Farquhar, 1982; Rinne et al., 2015) rose immediately after the selection harvest. This observation suggests a 38 % increase in a photosynthetic rate at stand scale, assuming that vapour pressure within the canopy airspace was unaffected, given that the water supply from a drained peatland soil was not reduced (Lehtonen et al., 2023b). This points to the fact that released Norway spruce trees preferentially allocate photosynthesised carbon into other plant parts after the selection harvest. However, such immediate increase in carbon allocation to support both crown and root system expansion as trees adjust to the new environment created by reduced stand density has rarely been investigated.

According to the functional balance theory (Garnier, 1991; Shipley and Meziane, 2002), increased irradiance shifts the allocation to roots (Poorter et al., 2012). Further, based on the allometric theory, there is isometrical scaling between the stem and root mass (Niklas, 2005), reflecting a balanced water delivery in the sapwood of coarse roots and stems. However, allometric scaling can also be derived from the mechanical theory, which shows that trees avoid uprooting by developing a counter-resisting force with a mechanically strong root system (Niklas and Spatz, 2006). Consistent with the functional balance theory and the allometric theory, it has been shown that white spruce (*Picea glauca*) trees allocate more carbon to roots soon after road construction next to their position in a forest (Urban et al., 1994). Similarly, retention cutting in Quebec increased the growth of coarse roots of residual black spruce (*Picea mariana*) trees before responses in stems, presumably due to increased light availability or to ensure mechanical support (Pretzsch et al., 2014). Indeed, both the tree structure (allometric scaling theory) and environmental factors (functional balance theory) can explain just as well the coarse-scale biomass partitioning between shoots and roots (Mccarthy and Enquist, 2007) because trees require both biomechanical stability and physiological equilibrium (Wang et al., 2023).

Selection harvesting affects the radiation conditions and microclimate within the forest canopy. The immediate post-harvest effect is greater light intensity on leaf surfaces of residual trees (especially those who had resided in suppressed positions), greater total radiation load and higher within-canopy wind velocity (Tikkasalo et al., 2024). In combination, surface and air temperatures within the canopy increase, which drives higher vapour pressure deficit and stronger canopy coupling with the atmosphere (Kim et al., 2014). Furthermore, although lower leaf area index decreases stand-scale transpiration (Tor-ngern et al., 2017), increased irradiance below the canopy will enhance soil and forest-floor evapotranspiration, partially negating the decrease in transpiring leaf area (Leppä et al., 2020b). When suppressed Norway spruce trees encounter these changes after harvest, their needles are still structurally adjusted to shade conditions and thus have low maximum stomatal conductance typical for shade leaves (Schulze et al., 1977). The actual conductance of the needles may decrease further below the maximum conductance due to the increased vapour pressure deficit (Oren et al., 1999). Thus, enhanced light intensity drives a higher CO_2 assimilation rate, leading to increased iWUE and increased stand-level WUE. On the other hand, an increase in VPD leads to higher transpiration rate and lower stomatal conductance which compensate the increase in iWUE and WUE. This compensating mechanism can also decrease the iWUE following thinning (Manrique-Alba et al., 2020). Furthermore, the root system of suppressed individuals is minimal horizontally and, thus, may not be able to take advantage of increasing water availability at the site or uptake nutrients in quantities sufficient to meet faster growth afforded by the higher carbon fixation. Thus, arguments can be posited for an immediate increase in carbon allocation to both aboveground, to foliage and stems and their mechanical support in the soil (proximal coarse root sections), and belowground, to distal coarse roots reflecting increasing transport capacity for soil resources necessary to meet the demand for greater photosynthesis.

Suppressed trees present a small silhouette positioned relatively close to the ground. Thus, a gradual increase in the cross-sectional area at the base of the stem and *proximal* section of the coarse roots may suffice for support against the increasing wind shear. Furthermore, not only do needles produced in the shade have low maximum conductance, but the long lifespan of Norway spruce needles means that shade foliage will be only slowly replaced by sun foliage with higher conductance (Zimmermann et al., 1988). Shade foliage also may keep transpiration rates low, making sapwood cross-sectional area sufficient to support the transpirational demand, at least until a large fraction of the foliage is replaced. However, a potentially small increase in transpirational demand means that only a small and gradual increase in belowground allocation to *distal coarse root* sections would suffice, especially if coupled with somewhat higher soil moisture after harvest, which is due to lower canopy interception and due to lower evapotranspiration (Leppä et al., 2020a). Indeed, the slow increase in stem growth may reflect a smaller than the presumed increase in carbohydrate availability because the increase of VPD would permit a smaller enhancement of photosynthetic rate than the 38 % suggested by iWUE (Lehtonen et al., 2023b).

Increment of cross-sectional area is an accurate representation of volume increment per unit of stem or root length. However, volume increment may be a poor representation of carbon available for biomass production because a given volume increment comprised of higher density wood represent greater carbon investment in production than that of low wood density. Thus, a treatment which increases volume increment rate may not reflect more carbon available for growth, especially considering that faster growing individuals often produce wood of lower density (Jaakkola et al., 2005). Weighing cross-sectional increment rate with wood density is an approach to represent biomass production (per unit length), combining treatment effects on both volume increment and wood density

Based on the synopsis above, two contrasting hypotheses can be formulated. The first is that the process of the progressive switch to sun foliage and higher leaf area slowly increases carbohydrate availability and balanced growth of all plant parts; thus, the delay in stem growth in response to opening the canopy simply reflects the difficulty in quantifying relatively small diameter increment on the background of natural variation. If so, enhancement of growth of both stems and coarse roots at proximal and distal locations would be difficult to detect for several years post-disturbance (**H1**). Alternatively, the enhancement of crown-scale carbohydrate production is considerable, but the stem capacity to transport water is sufficient over the following years. Thus, the extra carbohydrates produced are used in an immediate increase of allocation belowground to either shore up the tree against increasing winds, provide the canopy with more water, or both. Furthermore, the need for greater stability against increasing wind pressure manifests immediately, while the need for greater water uptake to support a high stomatal conductance occurs with delay due to a large fraction of shade foliage and due to increased water availability. A further hypothesis can be posited that proximal roots growth enhancement would be observable prior to that of distal roots (**H2**).

Here, we investigated the cross-sectional area growth of stems, proximal roots (next to the stump), and distal roots (1–1.5 m distance from the stem) to quantify the carbon allocation of suppressed Norway spruce trees after the selection harvest. To have a full picture related to carbon allocation to roots, we quantified the wood density of proximal and distal roots before and after selection harvest. We also quantified the lags of measurable increase in carbon allocation after the selection harvest at these three plant parts, determining the fate of extra carbon assimilated following the harvest. Because the secondary growth of Norway spruce is not particularly fast, we relied on laser ablation-based $\delta^{13}C$ detection (Saurer et al., 2023) to qualitatively obtain an early sign of a lag in new carbon allocation along the secondary xylem of roots. In earlier work, a lag between changes in $\delta^{13}C$ in stem and stem growth response allowed an earlier analysis to separate between the immediate onset of photosynthetic response and the delayed response of stem

growth (Lehtonen et al., 2023b). We then relied on analysis of growth along the pathway to both quantify lags and the strength of the response to help deduce which environmental drivers dominated early on and how strongly. We also wanted to understand how changes in the iWUE based on $\delta^{13}C$ measurements from stems and roots relate to model-based WUE estimates that also account for changes in the microclimate due to selection harvest.

2. Materials and methods

2.1. Study site

The study area was a drained peatland forest in Tammela, Lettosuo, in southern Finland (60° 38′ 31″ N, 23° 57′ 35″ E). The first ditches in this 18.5 ha area were dug in the 1930s, and more intensive drainage was carried out in 1969. The mean distance between ditches is 45 m, and their original depth was ~1 m. In March 2016, a 13-ha portion of the area was thinned by selection harvesting, and a small area (3.1 ha) was left unmanaged to serve as control. The site is fertile *Vaccinium myrtillus* type (Mtkg II) according to the classification of drained peatland sites (Vasander and Laine, 2008). Ground vegetation includes herbs, such as *Trientalis europaea* and *Dryopteris carthusiana*, and dwarf shrubs, such as *Vaccinium myrtillus* (Bhuiyan et al., 2017).

Before harvesting, the stand was dominated by naturally established mature Scots pine (*Pinus sylvestris*) trees with a small fraction of downy birch (*Betula pubescens*), while the lower canopy layer and the undergrowth were dominated by Norway spruce (Korkiakoski et al., 2023). Most trees shared one low canopy layer until the site was drained, but the stand had developed to a fully stocked mature stand with two canopy layers following drainage. Before the selection harvest, in both the control site and the area marked for selection harvest, mean tree height weighted by basal area was ~17 m for trees of all species, but it was ~20 m for the dominating Scots pine trees, suggesting suppression of Norway spruce trees relative to other species (Korkiakoski et al., 2023). In the selection harvest area, all Scots pines and some of the large birch and spruce trees were removed across different diameter classes, corresponding to a removal of 74 % of the original total stem volume. After harvest, downy birch accounted for 58 % of the total volume and Norway spruce for 42 %. However, due to their relatively small size, the post-harvest stem number of spruce stems (763 per ha) was twice that of birch. A more detailed description of the site and the management activities can be found in Korkiakoski et al. (2023), (2017)

2.2. Environmental conditions

Data from the closest automated weather station of the Finnish Meteorological Institute, located at Jokioinen (~35 km northwest of the study site), were used to inspect the environmental conditions and their long-term variation. The mean annual temperature during the 12-year period before the root sampling was 5.6℃ (Table S1), which is 0.4℃ and 1.0℃ higher than the 1991–2020 and 1981–2010 climate normals (Jokinen et al., 2021; Pirinen et al., 2012), respectively. When inspecting the 2010–2022 period, the annual mean temperature varied within 3.6–7.3℃.

The annual mean precipitation sum in 2010–2012 (623 mm) was about the same as the mean precipitation sum in climate normal periods of 1981–2010 (627 mm) and 1991–2020 (621 mm) (Jokinen et al., 2021; Pirinen et al., 2012), meaning that there has been no significant long-term change in the annual rainfall in the past 50 years. In 2010–2022, annual precipitation ranged from 434 mm to 783 mm (Table S1). Annual maximum snow depth has been highly variable over the years (Table S1). The annual maximum snow depth in 2010–2022 varied within 2–54 cm, averaging at 29 cm, while the long-term climate normal values were 27 cm and 20 cm in 1981–2010 and 1991–2020, respectively. The harvest-induced changes in the water and energy balance at the site have been described in Leppä et al. (2020).

2.3. Sampling and microscopy of roots

Roots were sampled at the end of April 2022. The same trees that were sampled by Lehtonen et al. (2023b) for increment cores from breast height were re-sampled for root discs for 2010–2021. Breast height diameters and surrounding basal areas varied for sampled trees in control from 7.4 cm to 11.7 cm (30.3–43.5 m^2 ha^{-1}), while for selection harvest the corresponding measures were from 11 cm to 14.2 cm (25.4–30.6 m^2 ha^{-1} before harvest) during 2020. Detailed statistics and tree maps describing sample tree positions relative to surrounding trees can be found from the Supplementary material 1 by Lehtonen et al. (2023b). One supporting coarse root of each sample tree (five in control and five in selection harvest areas) was selected at the southern side of the stem, and discs (1–2 cm thick) were cut close to the stem, representing the proximal root location (with oval shape, indicating supporting function), and at the distance of 1–1.5 m from the stem, representing the distal root location (see Supplementary material Figs. S1 and S2). We did not want to extend the destructive root disc sampling for additional tree individuals, as it might have produced bias for long term eddy covariance monitoring of these experimental stands. Proximal sections of roots, located closer to the stem than a point in which root diameter switches from a linear fast decrease with distance to a linear slow decrease, can be assumed to serve trees' needs for water transport and mechanical support (Ennos, 2000). Distal roots, defined as those beyond that inflection point, serve nearly entirely for water (and nutrient) transport (Kalliokoski et al., 2008). The root discs collected from the control and the harvested areas were investigated with a digital microscope (Olympus DSX1000, Tokyo, Japan) to evaluate the yearly growth (Supplementary Material Figs. S3 and S4).

2.3.1. Root disc preparation, cross-sectional areas and preparation for $\delta^{13}C$ analysis

Root discs were washed of peat and soaked in water for at least four days to attain full hydration. Thereafter, the disc diameter was measured at both ends of each disc in two perpendicular directions, allowing estimation of root tapering. The irregular shape of the proximal roots (Fig. S1) did not permit estimating annual cross-sectional growth using ring width obtained along these two axes of diameter measurements. Thus, annual cross-section increments of both proximal and distal roots were digitalised to allow a more precise estimate of annual carbon investments in root growth. The root cross-sections were scanned with a high-resolution scanner, and the images were brought into ImageJ software, where a scale on the images allowed the pixel area-to-cm^2 area ratio to be determined. Following this, we estimated the entire cross-sectional area of the root discs by manually delineating the outermost boundary of the most recent annual ring, and the area produced annually was estimated by delineating the outer boundary of each ring and calculating the difference in area between consecutive boundaries. This process was repeated until the ring representing the cross-sectional area in 2009 was identified, at which point the total cross-sectional area was measured again, defining the starting cross-sectional area for the analysis to have a cross-sectional area at the beginning of the 2010 growing season to have data from 5 growing seasons before selection harvesting.

The wood density of the root discs was measured with the QTRS-01X microdensitometer (Quintec Measurement Systems, Knoxville, USA) for 2000–2021. From the larger end of the air-dried discs, 1.6 mm thick wedges were sawn out in two perpendicular directions and scanned at a resolution of 0.02 mm. Time series for distal roots in control area starts from 1999, while for selection harvest area it starts from 1987 and data for proximal roots in control area start from 1991, while for selection harvest area they start from 1981. The mean wood density values for the annual rings were calculated from the continuous density profiles and are presented since 2000 (for further details, see the Supplementary Material, Table S2 and Fig. S5).

2.4. Carbon isotope composition of the wood

From the proximal root sections, an approximately 5 mm wide straight lath was cut from the pith to the edge of each disc for the carbon isotope analysis. The laths were cut systematically so that they were taken from the upper part of the roots relative to the soil surface. The direction of the cutting was selected in such a way that most of the ring boundaries were perpendicular to the long edge of the laths. This was done to ensure that ring borders were close to a 90-degree angle against the lath's long edge, although this was not always the case due to the complex shape of the root discs (Fig. S1). The smaller, distal root sections (Fig. S2) fit into the laser cell and were not cut prior to analysis. Next, the root sample sections were used to analyse the intra-annual variation in $\delta^{13}C$ values by laser ablation isotope ratio mass spectrometry (LA-IRMS) (Saurer et al., 2023). The LA-IRMS approach allowed quantification of intra-annual $\delta^{13}C$ variability in root growth rings without the need for tedious manual ring splitting, providing a more efficient alternative to conventional methods for high-resolution analysis. It also enabled the analysis of very narrow rings (13 μm), which would have been difficult or impossible to analyse using conventional methods (Loader et al., 2017; Saurer et al., 2023). The approach has been successfully applied to study the impact of forest management intervention on stem $\delta^{13}C$ values at the same location by Lehtonen et al. (2023b). Prior to LA-IRMS analyses, ethanol-soluble extractives (especially resins) were removed by boiling in ethanol for 48 h in a Soxhlet device, followed by rinsing with boiling MilliQ water for 6 h. The samples were left to dry at room temperature.

To account for intra-annual variation of $\delta^{13}C$, where the width of the ring allowed, five LA-IRMS measurements were taken, evenly distributed over the ring (e.g., the first measurement at the start of the ring, third at the mid-point, fifth at the end of the ring). The width of the laser track was 40 μm (laser ablation spot size), and the laser was run over a 0.9 mm long track along the ring; in the case of very narrow rings, a 30 μm spot size was used over a track length of 1.2 mm. Details of the analysis method can be found in Lehtonen et al. (2023b). The results were calibrated against USGS-55 reference material ($\delta^{13}C = -27.13$ ‰) and in-house reference yucca plant material ($\delta^{13}C = -15.46$ ‰), which were analysed concurrently with the samples. Both standards were homogenised powders that have been pressed into small discs using a manual hydraulic press. Repeated measurements of IAEA-C3 cellulose paper (International Atomic Energy Agency) were used as a quality control. When analysed concurrently with the samples, their measured $\delta^{13}C$ value was -24.73 ± 0.14 ‰ ($n = 212$; expected $\delta^{13}C = -24.91 \pm 0.49$ ‰). The samples' $\delta^{13}C$ results were corrected for changes in the $\delta^{13}C$ of atmospheric CO_2 (See Supplementary Material Table S3) based on the approach by McCarroll and Loader (2004).

2.5. Statistical analysis of the root rings

2.5.1. Testing prioritisation of C allocation: roots vs. stem

We first tested the potential time lag in the impact of the selection harvest on the cross-sectional area change of proximal and distal roots, as well as the stem, using a Before–After, Control–Impact (BACI) approach (e.g., Stewart-Oaten and Bence, 2001). This was based on mixed linear models of the relationship between the logarithm of the current cross-sectional area and the logarithm of its next year's annual increase (Pinheiro et al., 2017):

$$\log\left(y_{ijt}\right) = \mu + \eta\log\left(x_{ijt}\right) + \alpha_i + \beta_t + \gamma_{it} + u_{ij} + e_{ijt}, \quad (1)$$

where y_{ijt} is the difference in the cross-sectional area of tree j from area i (selection harvest or control) between years $t+1$ and t and x_{ijt} is the cross-sectional area in year t. Parameter α_i accounts for the difference between areas before the impact of the selection harvest (fixed to 0 for the control area and estimated as constant α for the selection harvest), parameter β_t is the overall change between periods before and after the impact (fixed to 0 for years t before the impact and estimated as constant β for years t after the impact in both areas), and γ_{it} accounts for the actual impact of the harvest (interaction of area and period effects; estimated as constant γ for trees from the selection harvest after the impact set to 0 for control and before the impact). The residual variation was divided into variability between trees (random effect u_{ij} with mean 0 and variance σ_u^2) and variability between repeated measurements of one tree (random effect e_{ijt} with mean 0 and variance σ_e^2).

To study the time lag in the impact, we fitted several versions of model (1) with different "first years of impact" T so that years $t < T$ were included in the "before impact" period and years $t \geq T$ to the "after impact" period. The tested values of T were 2016, 2017, …, 2020, i.e., 0–5 growing seasons after the selection harvest; models associated with different values of T were compared using the Akaike information criterion (AIC).

The impact of selection harvest on the stable carbon isotope ratio $\delta^{13}C$ was analysed in a similar manner to a model,

$$\delta^{13}C_{ijt} = \mu + \alpha_i + \beta_t + \gamma_{it} + u_{ij} + e_{ijt}, \quad (2)$$

where $\delta^{13}C_{ijt}$ is a weighted mean of $\delta^{13}C$ measurements from the year t ring of tree j from area i. The weights were determined according to the portions of the area of the ring represented by each spot (see Supplementary Material Fig. S6).

2.5.2. Testing if more C is allocated to distal roots compared to proximal roots

The impact of the selection harvest on basal area growth of proximal and distal roots was quantified by computing the predictions of relative growth at the selection harvest,

$$\widehat{g}_t = \frac{\widehat{y}_{\text{harvest},t}}{x_t} = \frac{1}{x_t}x_t^{\eta}\exp(\mu + \alpha + \beta_t + \gamma_{\text{harvest},t}) \quad (3)$$

from model (1), both before and after the impact ($\beta_t = 0$ and β, respectively). In these predictions, the current basal area x_t was set to the median value for the year 2016 at the selection harvest site (27.3 cm^2 for proximal and 0.67 cm^2 for distal roots).

2.6. Process-based model estimates for WUE and iWUE change

We estimated the changes in stand WUE and iWUE from the pyAPES model simulation results presented in Tikkasalo et al. (2024). In short, the effect of the harvest was simulated with the pyAPES model (Launiainen et al., 2022, 2015; Leppä et al., 2020b) for the years 2010–2020. pyAPES is a one-dimensional process-based soil-vegetation-atmosphere transfer model that can simulate the transfer of momentum, energy, CO_2 and H_2O in the vertical direction. The main driving forces in the model are the top-of-canopy meteorological conditions and the vertical leaf area distribution from which the model calculates the microclimatic gradients in the canopy.

In Tikkasalo et al. (2024), pyAPES was used to quantify the change in, e.g., stand microclimate, assimilation, stomatal conductance and transpiration due to changes in stand leaf area distribution following the harvest. Here, we utilised the same simulation results to calculate the change for the studied individual trees and stands in photosynthetically active radiation (PAR), net CO_2 assimilation (A_{net}), transpiration, VPD, effective stomatal conductance (g_{eff}), which is the inverse of the sum of reciprocals of stomatal and boundary layer conductance and the gross primary production (GPP) of a stand. From these variables, we also calculated the change in WUE and iWUE by dividing the change in A_{net} by transpiration and g_{eff}, respectively. We considered only the mean change in the variables on each studied stand for the years prior to the harvest (2010–2015) or after the harvest (2016–2020) and report the variability between the stands.

2.6.1. iWUE change estimate from change of $\delta^{13}C$

$\delta^{13}C$ of tree rings was converted to an iWUE estimate using the simple $\delta^{13}C$ model (Farquhar et al., 1989),

$$\delta^{13}C_{tr} \approx \delta^{13}C_{atm} - a - (b-a)\frac{C_i}{C_a} \quad (4)$$

where subindices tr refers to tree ring (either stem, distal or proximal roots) and atm means atmospheric. a (4.4 ‰) and b (27 ‰) are the fractionations associated with the diffusion of CO_2 through the stomata and RuBisCO fixation, respectively. C_i is the needle's internal CO_2 concentration and C_a the atmospheric CO_2 concentration. We estimated an average $\delta^{13}C_{atm}$ for the pre- and post-harvest periods using the weekly measured data from Pallas–Sammaltunturi GAW station (White et al., 2021).

Combining Eq. (4) with the definition of iWUE as the assimilation rate over the stomatal conductance for water and assuming that the assimilation is limited by the diffusion of CO_2 through stomata leads to the following:

$$\frac{iWUE_{post-harvest}}{iWUE_{pre-harvest}} = \frac{\delta^{13}C_{tr,post-harvest} - \delta^{13}C_{atm,post-harvest} + b}{\delta^{13}C_{tr,pre-harvest} - \delta^{13}C_{atm,pre-harvest} + b} \quad (5)$$

The pre- and post-harvest $\delta^{13}C$ values were calculated using Eq. (2), where the pre-harvest $\delta^{13}C$ is the sum of coefficients μ and α and post-harvest $\delta^{13}C$ is the sum of μ, α, β and γ.

3. Results

3.1. Carbon is allocated first to roots and then to stem after selection harvest

We found increased root growth starting immediately during the summer after the selection harvest (Supplementary Material Figs. S3–S4). Also, root carbon allocation was prioritised over stem carbon allocation. The best year of impact for the basal area growth model was found for the first year for proximal roots, the first and second years for distal roots, and the fourth year for the stem (Table 1). In contrast, the best year of impact for the $\delta^{13}C$ model was the first growing season after the selection harvest for all three plant parts. These findings refute **H1**, which assumed that it would be difficult to detect growth of stem and root cross-sections in several years after selection harvest. While results are not conclusive with **H2** due to fact that selection harvest induced growth increased with proximal roots during the first growing season and with distal roots during the first and second growing season.

The scaled cross-sectional increment for stem and roots showed that root growth was favoured over stem growth after the selection harvest. This is evidenced by a larger change in the cross-sectional increment of roots after the harvest compared to stems (Fig. 1 and Fig. S7 in Supplementary Material).

Over the first five years after the selection harvest, the relative growth of cross-sectional area increased fourfold for distal roots (4.08) and proximal roots (4.2), while the increase for stem was approximately two-fold, 2.03 (Fig. 1) compared to the five-year period before the harvest.

For the two types of root samples, we had estimates of wood density (Fig. S5), allowing us to generate an annual wood production index by combining the increased cross-sectional area with the wood density (Fig. 2). For distal roots in the selection harvest area, wood density was 40 % higher in 2010–2015 compared to the period before (2000–2009). However, for 2016–2021, wood density was decreased by 2 % from the 2010–2015 values. The trend was less pronounced for proximal roots; wood density was 10 % higher in 2010–2015 compared to the period before, and for 2016–2021, it decreased by 5 % from the 2010–2015 values (see Supplementary Material, Table S2 and Fig. S5). For the control site, the wood density of distal roots was 13 % higher for 2016–2021, compared to the period before, while wood density was 11 % higher for proximal roots during 2016–2021 compared to the period before.

Combining wood density information with the cross-sectional areas produces a biomass growth index (Fig. 2). This index shows that carbon allocation to roots increased during 2016 – 2019 for the selection harvest area, agreeing with the AIC analysis of the stem cross-sectional growth.

Table 1
AIC (Akaike information criterion) values for BACI models for cross-sectional area change and for $\delta^{13}C$ by tree parts: stem, proximal roots and distal roots. *T* indicates the starting year of the impact, and GS shows the number of growing seasons after the selection harvest. The lowest AIC values in bold indicate the first year of impact. For parameter values of the models, see Supplementary Material (Tables S5–S10).

T	GS	Basal area growth			$\delta^{13}C$		
		Stem	Proximal	Distal	Stem	Proximal	Distal
2016	1	426.1	**138.2**	265.4	**228.0**	**194.3**	**233.6**
2017	2	384.3	159.2	**265.2**	287.5	311.0	307.1
2018	3	338.5	191.9	289.1	331.1	346.5	342.1
2019	4	**331.9**	209.9	306.0	369.1	386.6	382.2
2020	5	430.2	215.9	316.2	388.0	409.0	406.7

3.2. Root and stem $\delta^{13}C$ values are in synchrony after treatment

Increased $\delta^{13}C$ was observed in the stems, proximal roots, and distal roots of the released spruce trees in the growing season following the selection harvest, indicating that the iWUE of these trees changed immediately under new conditions (Fig. 3 and Fig. 4).

The intra-annual patterns of $\delta^{13}C$ after the selection harvest were similar to those before the treatment for the three plant parts, indicating that carbon used for stems and roots after the selection harvest originated mostly from the current season's photosynthate and the use of reserves was marginal (Fig. 3). Intra-annual measurements of $\delta^{13}C$ in 2016 showed immediate increase in the $\delta^{13}C$ of roots and stem after the selection harvest compared to the values from the previous years, indicating also only minor reserve use (Fig. 3 and tables S5-S7).

The analysis of intra-annual (spot-level) $\delta^{13}C$ values showed that the difference between the minimum and maximum $\delta^{13}C$ values within each growing season was greater for roots after the selection harvest compared to the pre-harvest period (see Supplementary Material, Tables S8–S10 and Fig. 3).

The shift in $\delta^{13}C$ following the selection harvest is made apparent by converting the intra-annual values to annual values (Fig. 4, using data in Fig. 3, scaled with the approach shown in Fig. S6). The annual values show a tendency for stems to have higher iWUE than roots, especially in the control area. During 2016, there was an indication that proximal roots had the highest iWUE in the selection harvest area compared to stem and distal roots.

3.3. Increase in VPD after harvest leads to lower WUE increase compared to iWUE

Comparing the simulated WUE and iWUE revealed that WUE increases less than iWUE after the selection harvest (Fig. 5). After the harvest, within-canopy PAR, VPD and wind-speed increase due to reduced canopy leaf area. The positive effect of higher PAR on stomatal conductance more than compensates for the negative effect of VPD; furthermore, boundary layer conductance of needles also increases following the harvest. Higher conductance, together with the direct positive effect of PAR on the biochemistry of photosynthesis, leads to an increase in A_{net}. Nevertheless, the increase in A_{net} is higher than the increase in stomatal conductance due to increased VPD. The higher increase in A_{net} results in higher iWUE than WUE following the selection harvest.

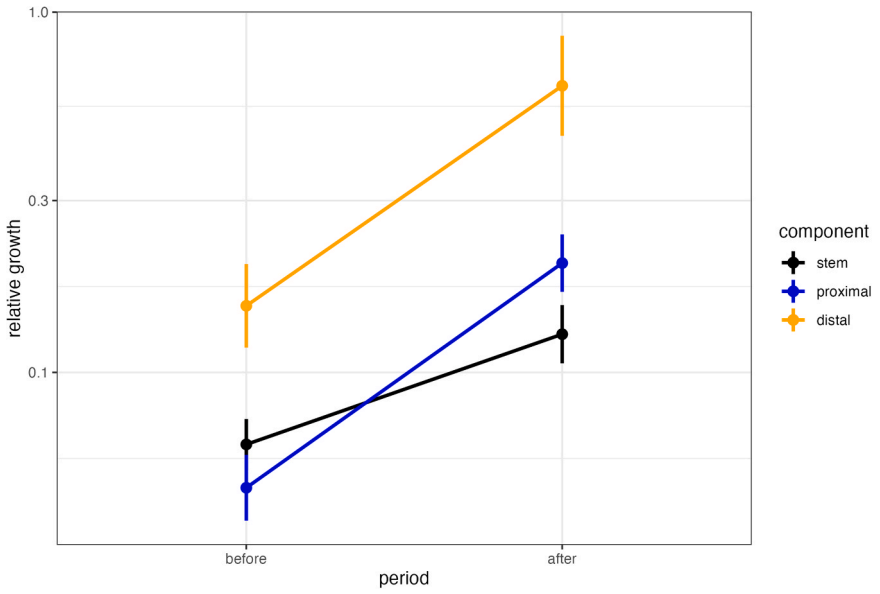

Fig. 1. Relative growth of stems and proximal and distal roots five years before and after the selection harvest. Root predictions are based on the median root diameter. Relative growth is based on the coefficients of the model presented in Eq. (3). Note the logarithmic scale of the y-axis.

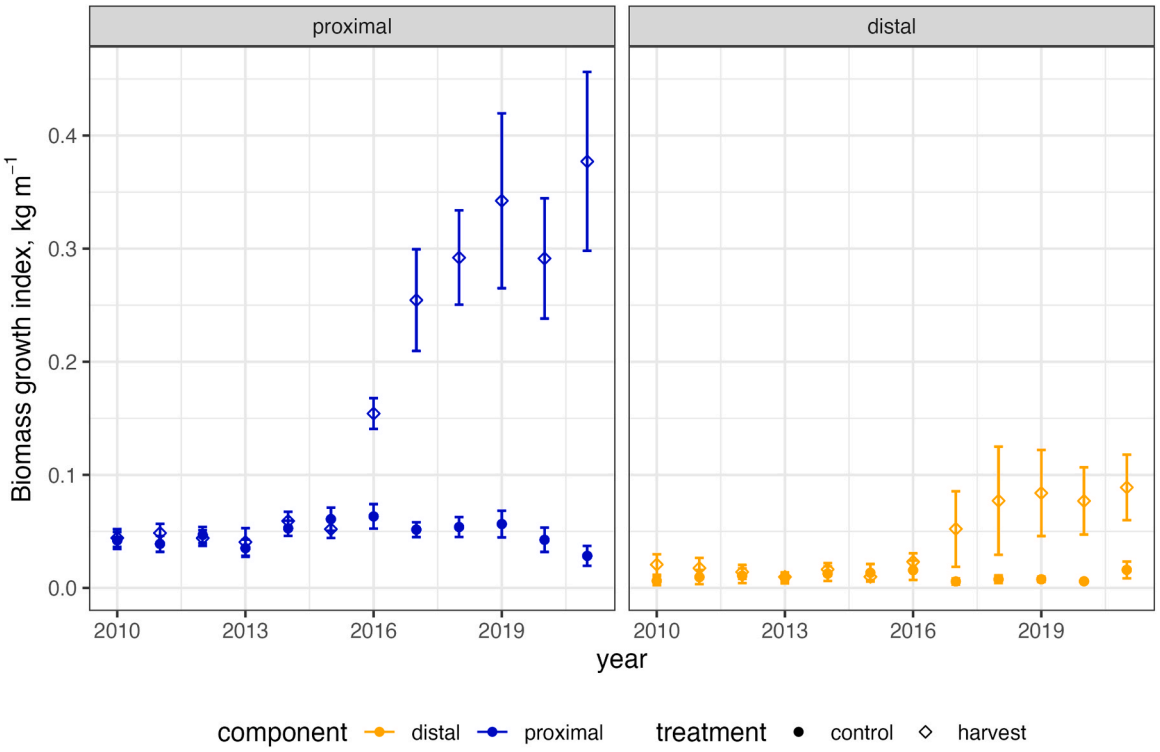

Fig. 2. Biomass growth index for the roots. The index has been derived by multiplying root cross-sectional increment areas (cm^2) with annual wood density estimates (kg m^{-3}). Error bars describe the standard error of the mean.

On the other hand, WUE is the ratio of photosynthesis over transpiration and, thus, reflects the effect of the harvest on transpiration, which is determined not only by its effects on g_{eff} but also on VPD. Following the harvest, VPD increases by a factor of approximately 1.23 (Fig. 5), and thus transpiration increases more than g_{eff}, leading to a smaller WUE increase compared to that of iWUE.

The measured iWUE values, showing approximately 46 % increase following the harvest are around the same as the simulated ones (approximately 58 %). Furthermore, the approximately 20 % lower mean GPP of the harvested area compared to the control, despite having 51 % lower leaf area index, is consistent with higher leaf-level productivity in the post-harvest area.

4. Discussion

4.1. Root growth increases immediately after selection harvest

Our results show that both proximal and distal roots increased their cross-sectional growth immediately following the selection harvest, refuting **H1** about minor changes in growth that are difficult to detect.

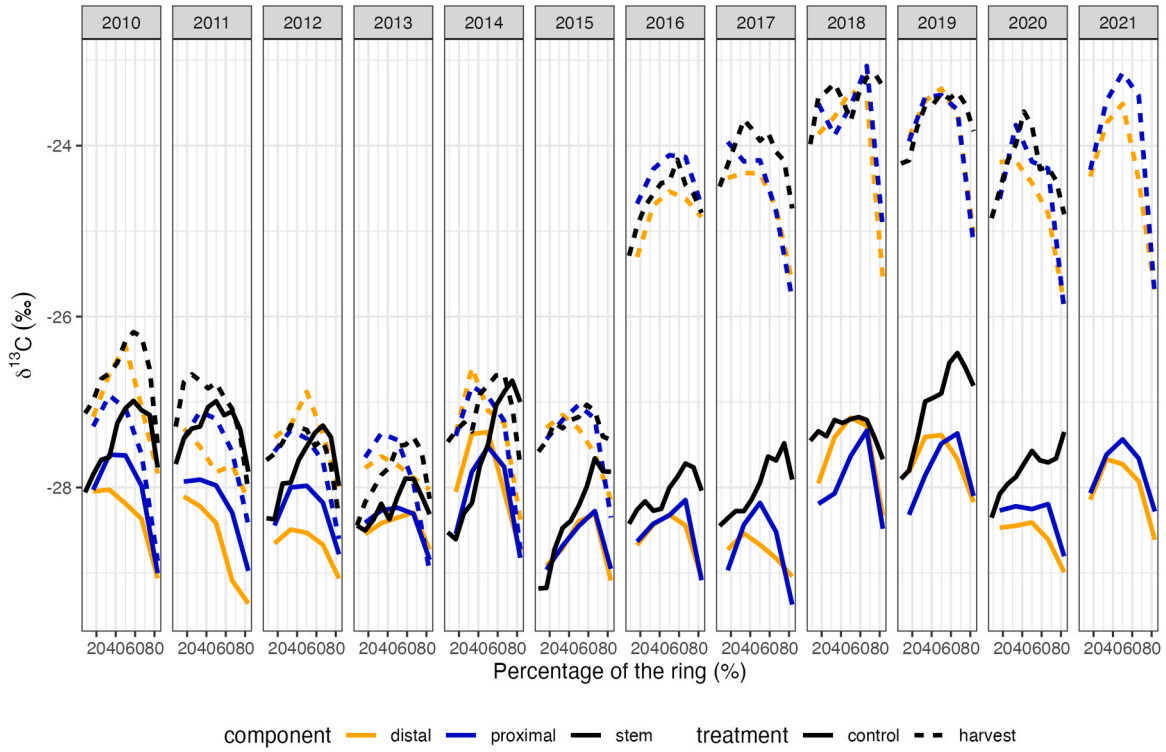

Fig. 3. $\delta^{13}C$ values for distal roots, proximal roots, and the stems (the latter from Lehtonen et al., 2023b) of Norway spruce for non-harvested (control) and selection harvesting (harvest) treatment areas, corrected for atmospheric $\delta^{13}C$ changes according to the relative position in the ring. Note that the stem measurements cover the period of 2010–2020, with 7–11 $\delta^{13}C$ data points per year, while root measurements cover 2010–2021 with five $\delta^{13}C$ data points per year.

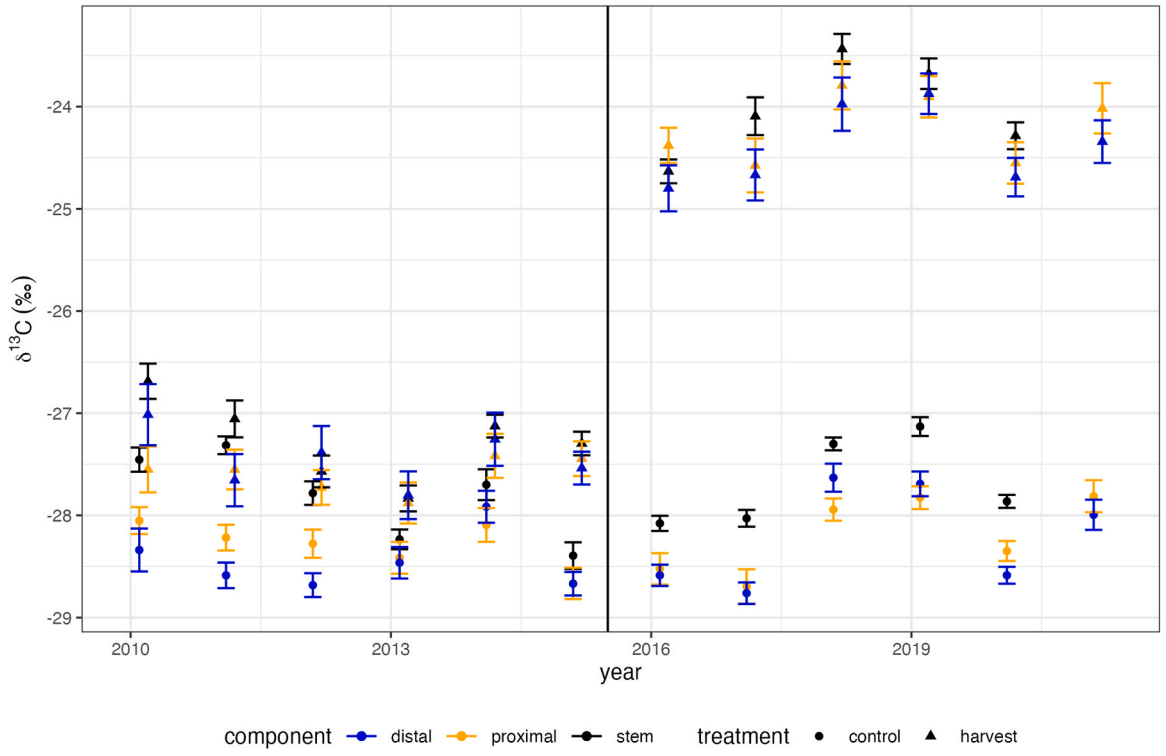

Fig. 4. Mean annual $\delta^{13}C$ values for the control and selection harvest areas for different tree parts (distal and proximal roots, and stems) before and after the selection harvest in 2016. Error bars describe the standard error of the mean, and the vertical line indicates the timing of the selection harvest.

These results demonstrate that the enhancement in carbohydrate production was sufficiently large to result in an observable growth response in the roots (Figs. 1 and 2). Unlike in roots, the growth response took four years to show up in stems, suggesting that stems presented neither a functional bottleneck to water transport nor a mechanical weak spot. Indeed, the immediate increase in proximal coarse root increment and a

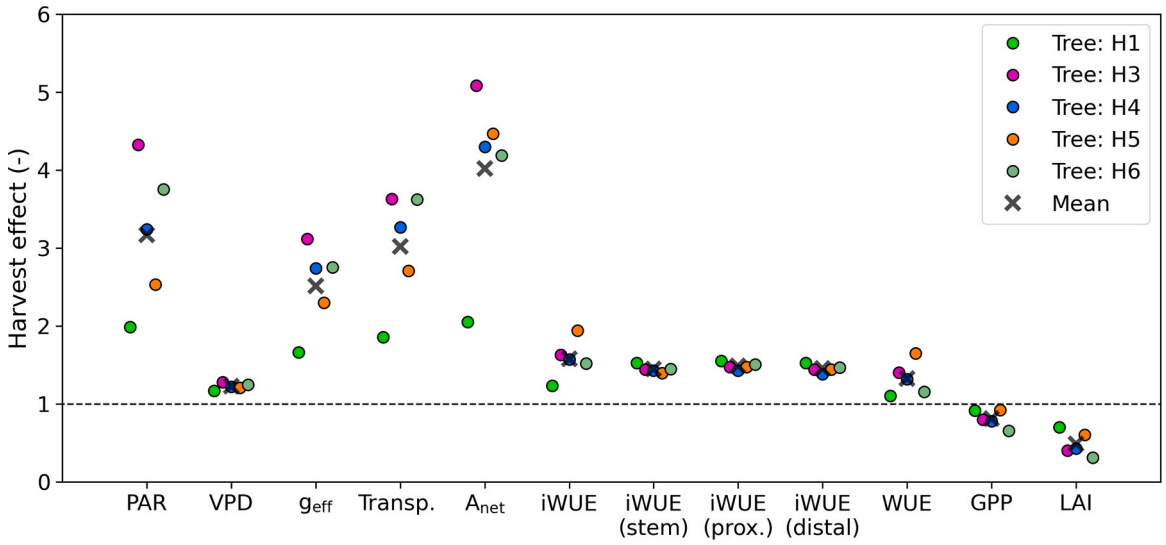

Fig. 5. Mean change in simulated variables according to Tikkasalo et al. (2024) between pre- and post-harvest periods for each tree. The black crosses show the mean change between all trees (and surrounding small stands). The variables are photosynthetically active radiation (PAR), water vapour pressure deficit (VPD), effective stomatal conductance (g_{eff}), transpiration (Transp.), stand-level net CO_2assimilation (A_{net}), intrinsic water use efficiency (iWUE), which is equal to assimilation divided by the effective stomatal conductance, water use efficiency (WUE), which is the assimilation divided by the transpiration, gross primary production (GPP) and leaf area index (LAI). All values were scaled per square metre of ground area before harvest effect calculation. Also shown are measured iWUE values calculated from the measured $\delta^{13}C$ of stems, distal- and proximal roots. Harvest effect (vertical axis) is the relative increase in the variable between pre- and post-harvest periods. Note that the model was run on each individual and its surrounding leaf area profile as an independent stand.

slightly delayed distal root increment (somewhat consistent with **H2**), both occurring two-to-three years before the increase in stem increment was observed, suggest that alleviation of mechanical anchoring belowground and quickly following water uptake limitations were more urgent.

These results are consistent with those from the very few studies exploring the dynamics of root and stem increments in response to reduced competition. Thinning of a Canadian black spruce stand resulted in growth enhancement of roots preceding that of stems by four years (Vincent et al., 2009). According to Nikolova et al. (2021), strip cutting in the Swiss Alps triggered higher growth in roots compared to that in stems of Norway spruce trees close to stand edges for two years after cutting, lasting for seven to eight years. Also, retention cutting in another black spruce stand (Quebec, Canada) increased the growth of coarse roots more than that of stems for the first five years, after which trees adapted to their new environment (Pretzsch et al., 2014).

We found that the relative growth enhancement in roots was approximately twice than that in stems, but it was similar in proximal and distal roots (Fig. 1). This observation suggests that investment in anchoring and uptake required similar relative increases in carbon allocation, and those investments were higher than the investment in stem water transport. Considering the higher g_{eff} and transpiration per unit of leaf area following the selection harvest, more water must be transported per unit of sapwood area, suggesting that the recently produced stem cross-sectional area is of higher capacity for water transport. This would be consistent with the difference observed in wood density and stem hydraulic conductance of slow versus fast-growing trees (Pothier et al., 1989). The finding that trees allocate more carbon to roots compared to stems after the selection harvest is a feature that is not captured in most empirical- and process-based models. When optimising forest practices for carbon uptake with models, our results demonstrate that it is important to include the production of both above- and belowground plant parts.

4.2. Selection harvesting triggers higher photosynthetic rate

Our results show that $\delta^{13}C$ increased immediately after the selection harvest in woody roots, as previously reported for stems of the same trees (Lehtonen et al., 2023b). Considering that carbon reserves formed prior to the harvest likely had a lower $\delta^{13}C$ signature and that the rise in $\delta^{13}C$ was similar in all three plant parts (increasing between 2.9 ‰ and 3.3 ‰ among different biomass components in the treated area), it seems that Norway spruce growth and its response to selection harvest is visible as an increase in the current season's assimilates, and these seem to be preferentially allocated to root production.

The change in $\delta^{13}C$ (i.e. iWUE) following the selection harvest was substantially greater in our study than observed in other studies. A synthesis of published results showed discrimination due to thinning to range between 1 ‰ and –0.4 ‰ based on increment cores from several *Pinus* species, Douglas fir (*Pseudotsuga menziesii*) and giant sequoia (*Sequoiadendrum giganteum*) along precipitation gradients (Marshall et al., 2022). The stronger effect (less discrimination) observed in the present study is likely due to these suppressed Norway spruce trees having been severely shaded under moist, nutrient-rich conditions and then suddenly released by the selection harvest, increasing the available PAR by approximately 220 % (Tikkasalo et al., 2024).

Furthermore, our results show that the stem $\delta^{13}C$ values were higher than those in roots, especially in the control area during most of the study years from 2010 to 2020 (Fig. 3). However, after the selection harvesting for 2016, there was an indication that distal root $\delta^{13}C$ values were higher than those for the stem. This observation indicates that the changed environmental conditions may have affected post-photosynthetic metabolic processes and the associated carbon isotope fractionation (Rinne-Garmston et al., 2023) and/or the timing and priority of carbon allocation to different plant parts.

4.3. Selection harvest increases water use efficiency

We found that the WUE (modelled 33 %) increases less than the iWUE (measured 46 %, modelled 58 %) after the selection harvest due to increased post-harvest VPD within the canopy. This finding highlights the importance of carefully accounting for all the changes in the forest microclimate when changes in tree processes in response to forest management practices are evaluated. Furthermore, our finding highlights the importance of not equating iWUE with WUE (e.g., Seibt et al., 2008; Siegwolf et al., 2022) because the first accounts for changes in the

driving force for photosynthesis and the latter also includes the change in the microclimate around the tree. For a more thorough understanding of how tree water usage changes after forest management operations, we recommend also measuring the change in VPD together with, e.g., $\delta^{13}C$ of tree rings, as VPD change can be used to estimate WUE from iWUE.

5. Conclusions

Our results show that net photosynthesis and biomass growth of suppressed Norway spruce trees respond positively and without delay to reduced competition after selection harvesting in the Lettosuo, fertile drained peatland. Additionally, the results from our study area demonstrate that trees allocate two times more carbon to root growth compared to stem growth in relative terms after the selection harvest. The data also show that Norway spruce increases carbon allocation to proximal and distal roots to a similar extent, highlighting the equal importance of mechanical support and nutrient and water transportation. This equal importance of root functions after the selection harvest may also result from the fact that young Norway spruce trees are known to be shade tolerant with a shallow root system and constrained allocation to roots.

Traditionally in forestry, observations of the delayed release effect have been based on stem diameter measurements and generalised to whole tree growth. However, our measurements of root cross-sectional growth showed an immediate and similar reaction to selection harvest in both proximal and distal roots. These findings underline the fact that selection harvests in fertile, drained peatlands provide immediate biomass growth and climate benefits at the tree level without any time lags. This finding also underlines the need to develop more appropriate carbon allocation routines for empirical and process-based models to account for the altered carbon allocation after the selection harvests. This is important, especially when those models are used to optimise forest practices according to the potential for climate change mitigation.

Authors' contributions

ALe, MP and RO planned and designed the study. ALe led the writing of the manuscript and conducted the statistical analysis with JH. OPT contributed to the analysis of the $\delta^{13}C$ results with a modelling approach and by estimating the relative changes of stand variables after the selection harvest. ES and GY contributed to the sample preparation and the LA-IRMS analysis. CB contributed by analysing the cross-sectional growth of root samples. MK provided the meteorological data for the analysis. YS, ALi, KRG and RO actively contributed to the interpretation of the data and results related $\delta^{13}C$ and tree physiology. All authors contributed to the writing process of the manuscript and gave final approval for publication.

CRediT authorship contribution statement

Mäkipää Raisa: Writing – review & editing, Funding acquisition, Conceptualization. **Rinne-Garmston Katja T:** Methodology. **Oren Ram:** Writing – review & editing, Writing – original draft, Investigation, Conceptualization. **Sahlstedt Elina:** Writing – original draft, Methodology, Data curation. **Korkiakoski Mika:** Writing – review & editing, Writing – original draft, Data curation. **Kärkönen Anna:** Writing – review & editing, Methodology, Data curation. **Lintunen Anna:** Writing – original draft, Investigation. **Mäkinen Harri:** Writing – review & editing, Methodology, Data curation. **Peltoniemi Mikko:** Writing – review & editing, Investigation, Data curation. **Lehtonen Aleksi:** Writing – review & editing, Writing – original draft, Visualization, Methodology, Investigation, Funding acquisition, Data curation, Conceptualization. **de Quesada Gonzalo:** Data curation. **Heikkinen Juha:** Writing – review & editing, Writing – original draft, Methodology. **Salmon Yann:** Writing – review & editing, Methodology, Investigation. **Boroski Chainey:** Software, Data curation. **Young Giles H.F.:** Writing – review & editing, Data curation. **Tikkasalo Olli-Pekka:** Writing – review & editing, Writing – original draft, Software, Methodology.

Declaration of Competing Interest

The authors declare that they have no known competing financial interests or personal relationships that could have appeared to influence the work reported in this paper.

Acknowledgements

We thank the field staff of the Natural Resources Institute Finland and the Finnish Meteorological Institute for contributing by collecting field data used in this study. The authors would like to thank the ICOS CP for providing the meteorological data used in this study. We would like to thank Natalia Kiuru for assistance in the sample preparation for the LA-IRMS analysis.

This work was supported by the Research Council of Finland funding for the BiBiFe project "Biogeochemical and biophysical feedbacks from forest harvesting to climate change" (nr. 325680) and by the Horizon Europe project FORWARDS "The ForestWard observatory to secure resilience of European forests" (nr. 101084481). KRG acknowledges funding from the European Research Council (ERC, 755865) and the Research Council of Finland (343059). ALi acknowledges funding by the Research Council of Finland "Managing forests for climate change mitigation" (347782, European Union – NextGenerationEU instrument), "Atmosphere and Climate Competence Center Research Flagship" (ACCC, 337549, 357902), "The role of bark in tree survival under drought stress" (355142).

Appendix A. Supporting information

Supplementary data associated with this article can be found in the online version at doi:10.1016/j.foreco.2025.122645.

Data Availability

Data is shared through Zenodo. LA-IRMS data analysed in the isotope laboratory of Natural Resources Institute Finland and stem- and root cross-sectional growth data of sample trees and R code for BACI analysis presented in this paper are available in Zenodo: 10.5281/zenodo.14046370. Meteorological data measured from the Lettosuo site at the central EC mast are available through the ICOS data portal (https://data.icos-cp.eu/) for 2017 onwards (Korkiakoski et al., 2024), while data for 2010–2016 is available from (http://icos-etc.eu/home).

References

Battipaglia, G., Saurer, M., Cherubini, P., Calfapietra, C., McCarthy, H.R., Norby, R.J., Francesca Cotrufo, M., 2013. Elevated CO_2 increases tree-level intrinsic water use efficiency: Insights from carbon and oxygen isotope analyses in tree rings across three forest FACE sites. N. Phytol. 197, 544–554. https://doi.org/10.1111/nph.12044.

Bhuiyan, R., Minkkinen, K., Helmisaari, H.-S., Ojanen, P., Penttilä, T., Laiho, R., 2017. Estimating fine-root production by tree species and understorey functional groups in two contrasting peatland forests. Plant Soil 412, 299–316. https://doi.org/10.1007/s11104-016-3070-3.

Ennos, A.R., 2000. The mechanics of root anchorage. In: Advances in Botanical Research. Academic Press, pp. 133–157. https://doi.org/10.1016/S0065-2296(00)33042-7.

Farquhar, G.D., Ehleringer, I.J.R., Hubick, K.T., 1989. Carbon isotope discrimination and photosynthesis. Annu. Rev. Plant. Biol. 40, 503–537.

Francey, R.J., Farquhar, G.D., 1982. An explanation of 13C/12C variations in tree rings. Nature 297, 28–31. https://doi.org/10.1038/297028a0.

Garnier, E., 1991. Resource capture, biomass allocation and growth in herbaceous plants. Trends Ecol. Evol. 6, 126–131.

Jaakkola, T., Mäkinen, H., Saranpää, P., 2005. Wood density in Norway spruce: changes with thinning intensity and tree age. Can. J. For. Res. 35 (7), 1767–1778.

Jokinen, P., Pirinen, P., Kaukoranta, J.-P., Kangas, A., Alenius, P., Eriksson, P., Johansson, M., Wilkman, S., 2021. Climatological and Oceanographic Statistics of Finland 1991–2020. Finnish Meteorological Institute. https://doi.org/10.35614/isbn.9789523361485.

Juutinen, A., Shanin, V., Ahtikoski, A., Rämö, J., Mäkipää, R., Laiho, R., Sarkkola, S., Laurén, A., Penttilä, T., Hökkä, H., Saarinen, M., 2021. Profitability of continuous-cover forestry in Norway spruce dominated peatland forest and the role of water table. Can. J. For. Res. 51, 859–870. https://doi.org/10.1139/cjfr-2020-0305.

Kalliokoski, T., Nygren, P., Sievänen, R., 2008. Coarse root architecture of three boreal tree species growing in mixed stands. Silva Fenn. 42. https://doi.org/10.14214/sf.252.

Kim, D., Oren, R., Oishi, A.C., Hsieh, C.-I., Phillips, N., Novick, K.A., Stoy, P.C., 2014. Sensitivity of stand transpiration to wind velocity in a mixed broadleaved deciduous forest. Agric. For. Meteorol. 187, 62–71. https://doi.org/10.1016/j.agrformet.2013.11.013.

Korkiakoski, M., Tuovinen, J.-P., Aurela, M., Koskinen, M., Minkkinen, K., Ojanen, P., Penttilä, T., Rainne, J., Laurila, T., Lohila, A., 2017. Methane exchange at the peatland forest floor – automatic chamber system exposes the dynamics of small fluxes. Biogeosciences 14, 1947–1967. https://doi.org/10.5194/bg-14-1947-2017.

Korkiakoski, M., Ojanen, P., Tuovinen, J.-P., Minkkinen, K., Nevalainen, O., Penttilä, T., Aurela, M., Laurila, T., Lohila, A., 2023. Partial cutting of a boreal nutrient-rich peatland forest causes radically less short-term on-site CO2 emissions than clear-cutting. Agric. For. Meteorol. 332, 109361. https://doi.org/10.1016/j.agrformet.2023.109361.

Korkiakoski, M., Aaltonen, H., Aurela, M., Hatakka, J., Laurila, T., Lohila, A., Rainne, J., Tuovinen, J., 2024. ETC L2 ARCHIVE, Lettosuo, 2016-12-31–2023-12-31.

Launiainen, S., Katul, G.G., Lauren, A., Kolari, P., 2015. Coupling boreal forest CO2, H2O and energy flows by a vertically structured forest canopy – Soil model with separate bryophyte layer. Ecol. Modell. 312, 385–405. https://doi.org/10.1016/j.ecolmodel.2015.06.007.

Launiainen, S., Katul, G.G., Leppä, K., Kolari, P., Aslan, T., Grönholm, T., Korhonen, L., Mammarella, I., Vesala, T., 2022. Does growing atmospheric CO $_2$ explain increasing carbon sink in a boreal coniferous forest? Glob. Change Biol. 28, 2910–2929. https://doi.org/10.1111/gcb.16117.

Lehtonen, A., Leppä, K., Rinne-Garmston, K.T., Sahlstedt, E., Schiestl-Aalto, P., Heikkinen, J., Young, G.H.F., Korkiakoski, M., Peltoniemi, M., Sarkkola, S., Lohila, A., Mäkipää, R., 2023b. Fast recovery of suppressed Norway spruce trees after selection harvesting on a drained peatland forest site. For. Ecol. Manag. 530, 120759. https://doi.org/10.1016/j.foreco.2022.120759.

Lehtonen, A., Eyvindson, K., Härkönen, K., Leppä, K., Salmivaara, A., Peltoniemi, M., Salminen, O., Sarkkola, S., Launiainen, S., Ojanen, P., Räty, M., Mäkipää, R., 2023a. Potential of continuous cover forestry on drained peatlands to increase the carbon sink in Finland. Sci. Rep. 13, 15510. https://doi.org/10.1038/s41598-023-42315-7.

Leppä, K., Korkiakoski, M., Nieminen, M., Laiho, R., Hotanen, J.-P., Kieloaho, A.-J., Korpela, L., Laurila, T., Lohila, A., Minkkinen, K., Mäkipää, R., Ojanen, P., Pearson, M., Penttilä, T., Tuovinen, J.-P., Launiainen, S., 2020b. Vegetation controls of water and energy balance of a drained peatland forest: Responses to alternative harvesting practices. Agr. For. Meteorol. 295, 108198. https://doi.org/10.1016/j.agrformet.2020.108198.

Leppä, K., Hökkä, H., Laiho, R., Launiainen, S., Lehtonen, A., Mäkipää, R., Peltoniemi, M., Saarinen, M., Sarkkola, S., Nieminen, M., 2020a. Selection cuttings as a tool to control water table level in boreal drained peatland forests. Front. Earth Sci. 8, 576510. https://doi.org/10.3389/feart.2020.576510.

Loader, N.J., McCarroll, D., Barker, S., Jalkanen, R., Grudd, H., 2017. Inter-annual carbon isotope analysis of tree-rings by laser ablation. Chem. Geol. 466, 323–326. https://doi.org/10.1016/j.chemgeo.2017.06.021.

Manrique-Alba, À., Beguería, S., Molina, A.J., González-Sanchis, M., Tomàs-Burguera, M., del Campo, A.D., Colangelo, M., Camarero, J.J., 2020. Long-term thinning effects on tree growth, drought response and water use efficiency at two Aleppo pine plantations in Spain. Sci. Total Environ. 728, 138536. https://doi.org/10.1016/j.scitotenv.2020.138536.

Marshall, J.D., Brooks, J.R., Talhelm, A.F., 2022. Forest management and tree-ring isotopes. In: Stable Isotopes in Tree Rings: Inferring Physiological, Climatic and Environmental Responses. Springer International Publishing, Cham, pp. 651–673.

McCarroll, D., Loader, N.J., 2004. Stable isotopes in tree rings. Quat. Sci. Rev. 23, 771–801. https://doi.org/10.1016/j.quascirev.2003.06.017.

Mccarthy, M.C., Enquist, B.J., 2007. Consistency between an allometric approach and optimal partitioning theory in global patterns of plant biomass allocation. Funct. Ecol. 21, 713–720. https://doi.org/10.1111/j.1365-2435.2007.01276.x.

Nieminen, M., Hökkä, H., Laiho, R., Juutinen, A., Ahtikoski, A., Pearson, M., Kojola, S., Sarkkola, S., Launiainen, S., Valkonen, S., Penttilä, T., Lohila, A., Saarinen, M., Haahti, K., Mäkipää, R., Miettinen, J., Ollikainen, M., 2018. Could continuous cover forestry be an economically and environmentally feasible management option on drained boreal peatlands? For. Ecol. Manag. 424, 78–84. https://doi.org/10.1016/j.foreco.2018.04.046.

Niklas, K.J., 2005. Modelling Below- and Above-ground Biomass for Non-woody and Woody Plants. Ann. Bot. 95, 315–321. https://doi.org/10.1093/aob/mci028.

Niklas, K.J., Spatz, H., 2006. Allometric theory and the mechanical stability of large trees: proof and conjecture. Am. J. Bot. 93, 824–828. https://doi.org/10.3732/ajb.93.6.824.

Nikolova, P.S., Geyer, J., Brang, P., Cherubini, P., Zimmermann, S., Gärtner, H., 2021. Changes in root–shoot allometric relations in alpine Norway spruce trees after strip cutting. Front. Plant Sci. 12, 703674.

Oren, R., Sperry, J.S., Katul, G.G., Pataki, D.E., Ewers, B.E., Phillips, N., Schäfer, K.V.R., 1999. Survey and synthesis of intra- and interspecific variation in stomatal sensitivity to vapour pressure deficit. Plant Cell Environ. 22, 1515–1526. https://doi.org/10.1046/j.1365-3040.1999.00513.x.

Pinheiro, J., Bates, D., DebRoy, S., Sarkar, D., Heisterkamp, S., Willigen, B.V., Maintainer, R., 2017. Package 'nlme.' Linear and Nonlinear Mixed Effects Models, version 3–1.

Pirinen, P., Simola, H., Aalto, J., Kaukoranta, J.-P., Karlsson, P., Ruuhela, R., 2012. Tilastoja Suomen Ilmastosta 1981-2010.

Poorter, H., Niklas, K.J., Reich, P.B., Oleksyn, J., Poot, P., Mommer, L., 2012. Biomass allocation to leaves, stems and roots: meta-analyses of interspecific variation and environmental control. N. Phytol. 193, 30–50. https://doi.org/10.1111/j.1469-8137.2011.03952.x.

Pothier, D., Margolis, H.A., Poliquin, J., Waring, R.H., 1989. Relation between the permeability and the anatomy of jack pine sapwood with stand development. Can. J. For. Res. 19, 1564–1570.

Pretzsch, H., Heym, M., Pinna, S., Schneider, R., 2014. Effect of variable retention cutting on the relationship between growth of coarse roots and stem of *Picea mariana*. Scand. J. For. Res. 1–12. https://doi.org/10.1080/02827581.2014.903992.

Rinne, K.T., Saurer, M., Kirdyanov, A.V., Loader, N.J., Bryukhanova, M.V., Werner, R.A., Siegwolf, R.T.W., 2015. The relationship between needle sugar carbon isotope ratios and tree rings of larch in Siberia. Tree Physiol. 35, 1192–1205. https://doi.org/10.1093/treephys/tpv096.

Rinne-Garmston, K.T., Tang, Y., Sahlstedt, E., Adamczyk, B., Saurer, M., Salmon, Y., Carrasco, M., del, R.D., Hölttä, T., Lehmann, M.M., Mo, L., et al., 2023. Drivers of intra-seasonal δ13C signal in tree-rings of Pinus sylvestris as indicated by compound-specific and laser ablation isotope analysis. Plant. Cell Environ. 46, 2649–2666.

Saurer, M., Sahlstedt, E., Rinne-Garmston, K.T., Lehmann, M.M., Oettli, M., Gessler, A., Treydte, K., 2023. Progress in high-resolution isotope-ratio analysis of tree rings using laser ablation. Tree Physiol. 43, 694–705. https://doi.org/10.1093/treephys/tpac141.

Schulze, E.-D., Fuchs, M.I., Fuchs, M., 1977. Spacial distribution of photosynthetic capacity and performance in a mountain spruce forest of Northern Germany. Oecologia 29, 43–61. https://doi.org/10.1007/BF00345361.

Seibt, U., Rajabi, A., Griffiths, H., Berry, J.A., 2008. Carbon isotopes and water use efficiency: sense and sensitivity. Oecologia 155, 441–454.

Shipley, B., Meziane, D., 2002. The balanced-growth hypothesis and the allometry of leaf and root biomass allocation: *Allometry versus balanced growth hypotheses*. Funct. Ecol. 16, 326–331. https://doi.org/10.1046/j.1365-2435.2002.00626.x.

Siegwolf, R.T., Brooks, J.R., Roden, J., Saurer, M., 2022. Stable Isotopes In Tree Rings: Inferring Physiological, Climatic And Environmental Responses. Springer Nature, Switzerland.

Stewart-Oaten, A., Bence, J.R., 2001. Temporal and spatial variation in environmental impact assessment. Ecol. Monogr. 71, 305–339. https://doi.org/10.1890/0012-9615(2001)071[0305:TASVIE]2.0.CO;2.

Tikkasalo, O.-P., Leppä, K., Launiainen, S., Peltoniemi, M., Mäkipää, R., Rinne-Garmston, K.T., Sahlstedt, E., Young, G.H.F., Bokareva, A., Lohila, A., Korkiakoski, M., Schiestl-Aalto, P., Lehtonen, A., 2024. Modeling the response of Norway spruce tree-ring carbon and oxygen isotopes to selection harvest on a drained peatland forest. Tree Physiol. 44. https://doi.org/10.1093/treephys/tpad119.

Tor-ngern, P., Oren, R., Oishi, A.C., Uebelherr, J.M., Palmroth, S., Tarvainen, L., Ottosson-Löfvenius, M., Linder, S., Domec, J., Näsholm, T., 2017. Ecophysiological variation of transpiration of pine forests: synthesis of new and published results. Ecol. Appl. 27, 118–133. https://doi.org/10.1002/eap.1423.

Urban, S.T., Lieffers, V.J., Macdonald, S.E., 1994. Release in radial growth in the trunk and structural roots of white spruce as measured by dendrochronology. Can. J. For. Res. 24, 1550–1556. https://doi.org/10.1139/x94-202.

Vasander, H., Laine, J., 2008. In: Korhonen, Riitta, Korpela, Leila, Sarkkola, Sakari (Eds.), Site Type Classification On Drained Peatlands. Finnish Peatland Society Maahenki, Finland, pp. 146–151.

Vincent, M., Krause, C., Zhang, S.Y., 2009. Radial growth response of black spruce roots and stems to commercial thinning in the boreal forest. Forestry 82, 557–571. https://doi.org/10.1093/forestry/cpp025.

Wang, H., Qin, J., Hu, Y., Guo, C., 2023. Asymmetric growth of belowground and aboveground tree organs and their architectural relationships: a review. Can. J. For. Res. 53, 315–327. https://doi.org/10.1139/cjfr-2022-0216.

White, J., Vaughn, B., Michel, S., 2021. Flask-Air Sample Measurements of Stable Isotopic Composition of Atmospheric Carbon Dioxide (d13C-CO2) at NOAA GML Global and Regional Background Sites, 1990-Present (Version 2021-02-04) [Data set]. NOAA GML CCGG.

Zimmermann, R., Oren, R., Schulze, E.-D., Werk, K., 1988. Performance of two Picea abies (L.) Karst. stands at different stages of decline: II. Photosynthesis and leaf conductance. Oecologia 76, 513–518.